Supporting Information for:

EPR Study of UV-irradiated Thymidine Microcrystals Supports Radical Intermediates in Spore Photoproduct Formation

Ellen C. Hayes[†], Yajun Jian[‡§], Lei Li[‡], Stefan Stoll[†*]

[†] Department of Chemistry, Box 351700, University of Washington, Seattle, WA 98195
[‡] Department of Chemistry & Chemical Biology, 402 N. Blackford Street, LD 326, Indiana University – Purdue University Indianapolis (IUPUI), Indianapolis, IN 46202

Present Address:

[§] School of Chemistry & Chemical Engineering, Shaanxi Normal University (SNNU), No. 620, West Chang'an Avenue, Xi'an, Shaanxi, 710119, P. R. China

Table of Contents

1. Simulation parameters for EPR spectra

Table S1a: EPR parameters (g values and hyperfine coupling values) for simulations of TCH_2 isotopologues in Figure 1 [a,b,c,d]

	species	g	g frame	H_{C6}	H_{C6} frame	H_{C7}	H_{C7} frame	H_{C7}	H_{C7} frame	$^{14}N1$	$^{14}N1$ frame	LWPP [e] (mT)
DFT	TCH_2	2.0024 2.0029 2.0033	-66° 26° -42°	-49 -38 -15	17° 40° -36°	-75 -51 -19	138° 15° -162°	-70 -50 -18	166° 130° 148°	-4 5 -5	168° 101° -113°	N.A.
120K	TCH_2	2.0045 2.0055 2.0065	-66° 26° -42°	-36 -28 -20	17° 40° -36°	-56 -42 -19	138° 15° -162°	-56 -42 -22	166° 130° 148°	-1 -1 5	168° 101° -113°	0.6
	TCD_2	P	P	P	P	P·D	P	P·D	P	P	P	0.8
210K	TCH_2	P	P	P	P	P	P	P	P	P	P	0.7
	TCD_2	P	P	P	P	P·D	P	P·D	P	P	P	0.8
250K	TCH_2	P	P	P	P	P	P	P	P	P	P	0.6
	TCD_2	P	P	P	P	P·D	P	P·D	P	P	P	0.9

[a] All hyperfine values are in MHz
[b] "P" indicates the value is the same as the value for the primary isotopologue in the 3rd row of the table (TCH_2 at 120 K)
[c] $P{\cdot}D = P{\cdot}\,{}^{\gamma_{2_H}}/_{\gamma_{1_H}}$, D is the ratio of gyromagnetic ratios for ^2H and ^1H, approx. 0.1535
[d] All frames are the Euler angles of the rotation matrices computed in Orca
[e] Peak-to-peak line width

Table S1b: EPR parameters for simulations of TH isotopologues in Figure 1 [a,b,c,d]

	species	g	g frame	H_{C7} (methyl)	H_{C7} frame	H_{C6}	H_{C6} frame	H_{C6}	H_{C6} frame	LWPP[e] (mT)
DFT	TH	2.0023 2.0044 2.0056	142° 20° -66°	54 55 63	4° 82° 104°	58 59 70	86° 12° -69°	119 120 132	180° 43° -114°	N.A.
120K	TH	2.0021 2.0067 2.0080	142° 20° -66°	54 56 64	4° 82° 104°	114 114 117	86° 12° -69°	110 110 113	180° 43° -114°	0.6
	TD	P	P	P	P	P	P	P·D	P	0.4
	TH-d_3	P	P	P·D	P	P	P	P	P	0.3
	TD-d_3	P	P	P·D	P	P·0.75	P	P·D	P	0.3
210K	TH	P	P	P	P	P	P	P	P	0.7
	TD	P	P	P	P	P	P	P·D	P	0.4
	TH-d_3	P	P	P·D	P	P	P	P	P	0.6
	TD-d_3	P	P	P·D	P	P·0.75	P	P·D	P	0.7
250K	TH	P	P	P	P	P	P	P	P	0.5
	TD	P	P	P	P	P	P	P·D	P	0.5
	TH-d_3	P	P	P·D	P	P	P	P	P	1.0
	TD-d_3	P	P	P·D	P	P·0.75	P	P·D	P	0.7

[a] All hyperfine values are in MHz
[b] "P" indicates the value is the same as the value for the primary isotopologue in the 3rd row of the table (TH at 120 K)
[c] P·D =P· $\gamma_{2_H}/\gamma_{1_H}$, D is the ratio of gyromagnetic ratios for ^{2}H and ^{1}H, approx. 0.1535
[d] All frames are the Euler angles of the rotation matrices computed in Orca
[e] Peak-to-peak line width

2. Alternative model for EPR simulations of data in Figure 1

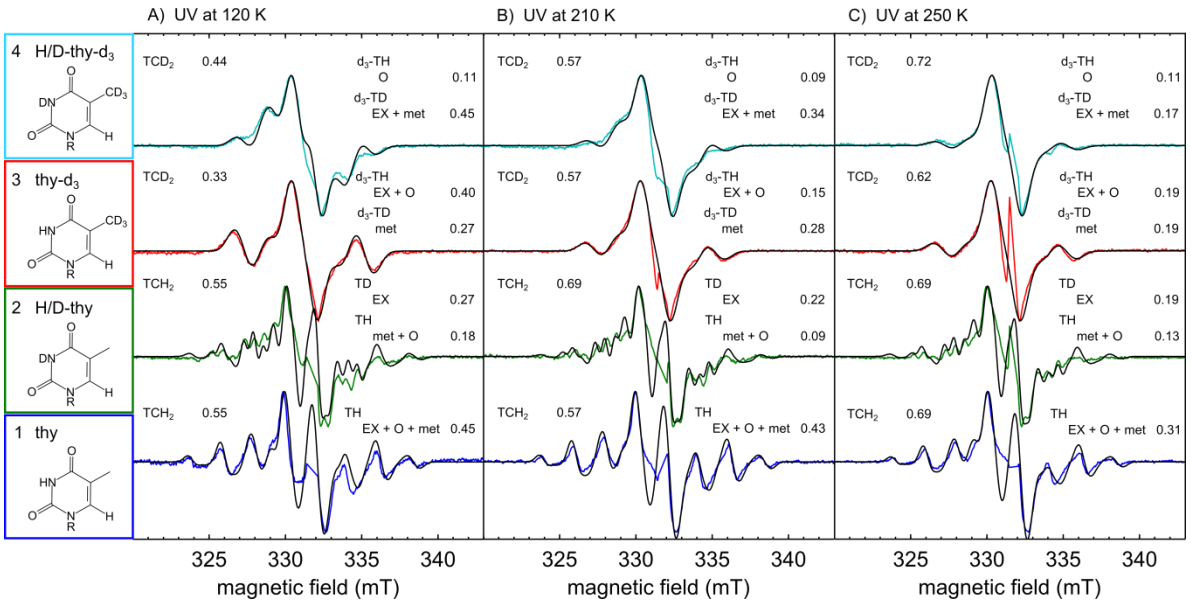

Figure S1. Continuous-wave EPR spectra collected at 120 K of microcrystalline powder samples of thymidine, H/D-thymidine, thymidine-d_3, and H/D-thymidine-d_3 photodamaged with 266 nm laser pulses at variable temperatures (120 K, 210 K, 250 K) indicated at the top of each set of axes (identical spectra to those presented in Figure 1 of the main text, see main text for additional experimental details). The structures of the starting materials are shown in the left column. The ratio of isotopologues of the TCH_2 and TH radicals that are used to simulate the spectra are indicated within the figure. In addition, the pathways ("met", "EX", or "O") that lead to a specific TH isotopologue for each starting material are indicated. In contrast to the simulations in Figure 1 of the main text, the simulations here do not assume the 1:1 restriction or the isotope effect restriction (defined in the main text). In all cases the spectra and simulations were normalized to their most intense feature for clarity. See main text (Discussion Section) for a discussion of the relevance of these simulations.

Table S2a: EPR parameters for simulations of TCH_2 isotopologues at variable temperatures in Figure S1 [a,b,c,d]

	species	*g*	g frame	H_{C6}	H_{C6} frame	H_{C7}	H_{C7} frame	H_{C7}	H_{C7} frame	$^{14}N1$	$^{14}N1$ frame	LWPP [e] (mT)
120K	TCH_2	2.0045 2.0055 2.0065	-66° 26° -42°	-36 -28 -20	17° 40° -36°	-56 -42 -19	138° 15° -162°	-56 -42 -22	166° 130° 148°	-1 -1 5	168° 101° -113°	0.7
	TCD_2	P	P	P	P	P·D	P	P·D	P	P	P	0.9
210K	TCH_2	P	P	P	P	P	P	P	P	P	P	0.8
	TCD_2	P	P	P	P	P·D	P	P·D	P	P	P	1.0
250K	TCH_2	P	P	P	P	P	P	P	P	P	P	0.8
	TCD_2	P	P	P	P	P·D	P	P·D	P	P	P	1.0

[a] All hyperfine values are in MHz
[b] "P" indicates the value is the same as the value for the primary isotopologue in the 2nd row of the table (TCH_2 at 120 K)
[c] P·D =P· $\gamma_{2_H}/\gamma_{1_H}$, D is the ratio of gyromagnetic ratios for ^2H and ^1H, approx. 0.1535
[d] All frames are the Euler angles of the rotation matrices computed in Orca
[e] Peak-to-peak line width

Table S2b: EPR parameters for simulations of TH isotopologues at variable temperatures in Figure S1 [a,b,c,d]

	species	g	g frame	H_{C7} (methyl)	H_{C7} frame	H_{C6}	H_{C6} frame	H_{C6}	H_{C6} frame	LWPP[e] (mT)
120K	TH	2.0021 2.0067 2.0080	142° 20° -66°	54 56 64	4° 82° 104°	114 114 117	86° 12° -69°	110 110 113	180° 43° -114°	0.6
	TH	P	P	P	P	P	P	P·D	P	0.4
	TD	P	P	P·D	P	P·0.95	P	P	P	0.6
	TH-d_3	P	P	P·D	P	P·0.80	P	P·D	P	0.5
210K	TD-d_3	P	P	P	P	P	P	P	P	0.6
	TH	P	P	P	P	P	P	P·D	P	0.4
	TD	P	P	P·D	P	P·0.95	P	P	P	0.6
	TH-d_3	P	P	P·D	P	P·0.75	P	P·D	P	0.6
250K	TD-d_3	P	P	P	P	P	P	P	P	0.6
	TH	P	P	P	P	P	P	P·D	P	0.4
	TD	P	P	P·D	P	P	P	P	P	0.7
	TH-d_3	P	P	P·D	P	P·0.75	P	P·D	P	0.7

[a] All hyperfine values are in MHz
[b] "P" indicates the value is the same as the value for the primary isotopologue in the 2[rd] row of the table (TH at 120 K)
[c] P·D =P· $\gamma_{2_H}/\gamma_{1_H}$, D is the ratio of gyromagnetic ratios for ^{2}H and ^{1}H, approx. 0.1535
[d] All frames are the Euler angles of the rotation matrices computed in Orca
[e] Peak-to-peak line width

3. Reproducibility of radicals produced in thymidine microcrystals and thin films exposed to UV radiation

3a. Spectra acquired after UV irradiation at 120 K

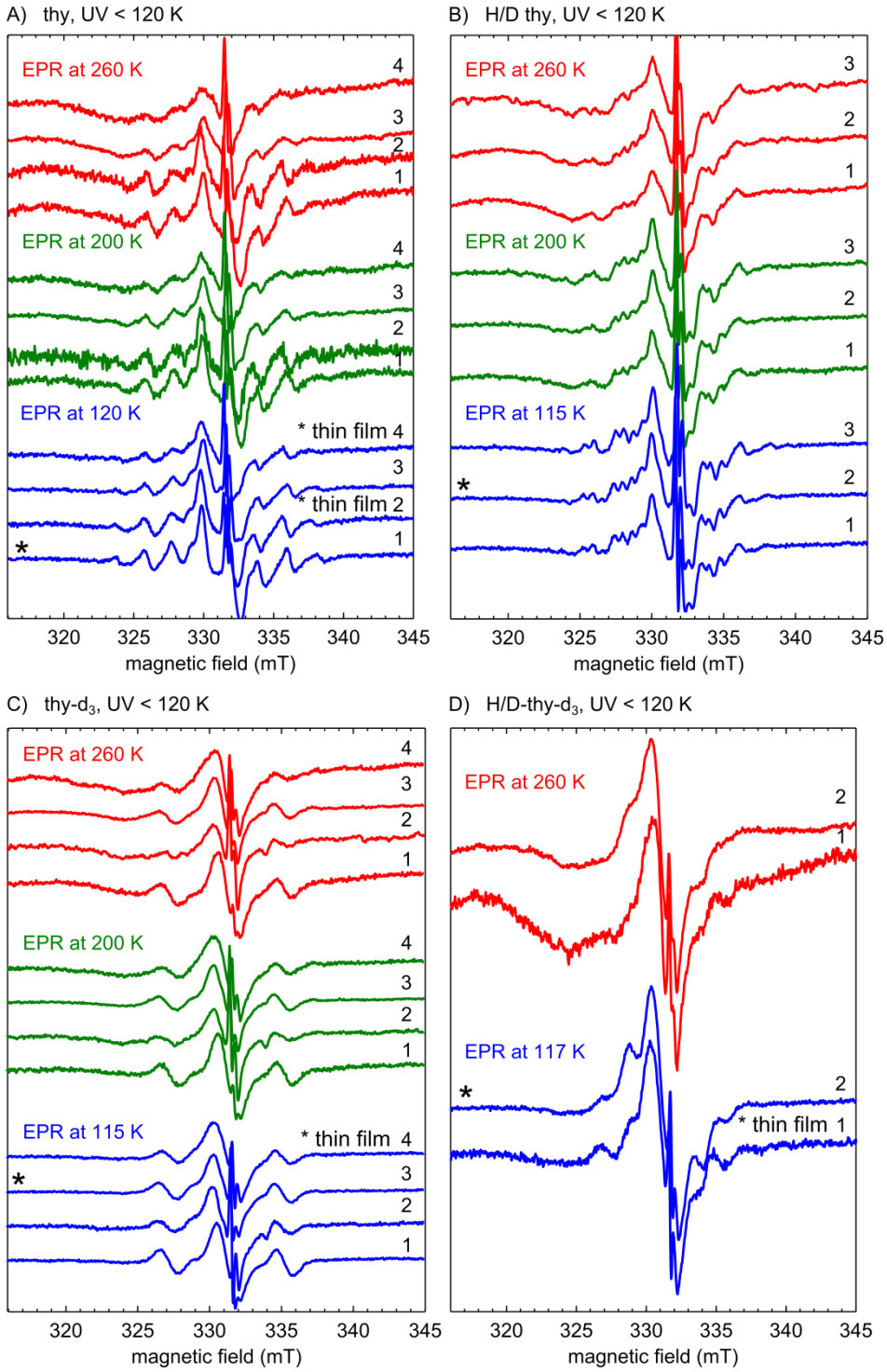

Figure S2. Multiple trials of UV irradiation (266 nm, 10 Hz, ≈ 30 min) at less than or equal to 120 K of thymidine, H/D thymidine, thymidine-d_3, and H/D thymidine-d_3. Within each figure (A, B, C, D), spectra marked with the same number are of the same sample but the temperature was raised in the EPR cavity from 120 K (blue), to 200 K (green), to 260 K (red) without removing the sample from the EPR cavity. Except where indicated, all samples are microcrystalline powder samples prepared as described in the main text. Thin film samples are prepared as described below. Spectrometer settings were as follows: microwave attenuation was 33 dB for spectra recorded below 120 K, greater than or equal to 25 dB for spectra recorded at 200 K, and greater than or equal to 20 dB for spectra recorded at 260 K; sweep rates of ≈ 40 seconds over 30 mT; microwave frequency near 9.3 GHz; modulation amplitude of 0.2 mT and frequency of 100 kHz; typically 30-100 scans were needed to achieve the signal to noise ratio of the spectra shown. Spectra marked with a star (*) are spectra shown in Figure 1 of the main article.

This figure shows that thin-film preparation of samples generally leads to broader features in the spectra. Thin-film samples 2 and 4 in Figure 2A, 4 in Figure 2C, and 1 in Figure 2D all have broadened features compared to their microcrystalline analogues. However, the yield of radical isotopologues of TCH_2 and TH does not appear to depend on the preparation between thin film and microcrystal.

3b. Spectra acquired after UV irradiation at 210 and 250 K

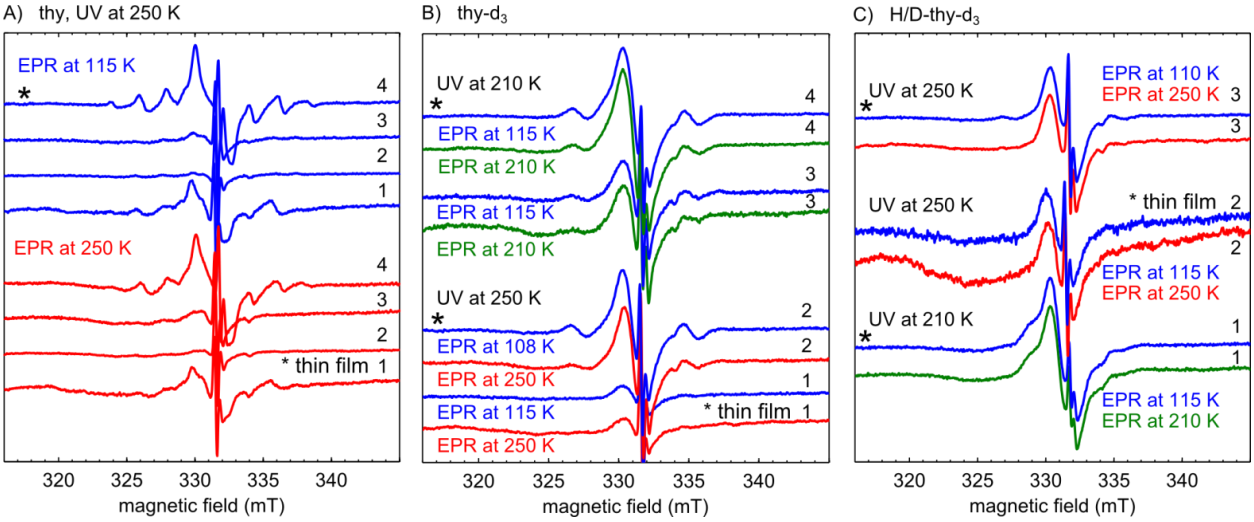

Figure S3: Multiple trials of UV irradiation (266 nm, 10 Hz, ≈ 30 min) at 210 K and 250 K of thymidine, thymidine-d_3, and H/D thymidine-d_3. Within each figure (A,B,C) spectra marked with the same number are of the same sample but the temperature was lowered in the EPR cavity from either 250 K or 210 K (red or green, respectively) to 120 K (blue) without removing the sample from the EPR cavity. Except where indicated, all samples are microcrystalline powder samples prepared as described in the main text. Thin film samples are prepared as described below. Spectrometer settings were as follows: microwave attenuation was 33 dB for spectra recorded below 120 K, greater than or equal to 25 dB for spectra recorded at 200 K, and greater than or equal to 20 dB for spectra recorded at 250 K; sweep rates of 40 seconds for 30 mT; microwave frequency near 9.3 GHz; modulation amplitude of 0.2 mT and frequency of 100 kHz; typically 30-100 scans were needed to achieve the signal to noise ratio of the spectra shown. Spectra marked with a star (*) are spectra shown in Figure 1 of the main article.

This figure shows that, once again, thin film preparation of samples generally leads to broader features in the spectra (compare thin film sample 1 in A to microcrystal sample 4 in A). Cooling both thin film and microcrystalline samples after UV irradiation always sharpens the features (especially sample 4 in A, samples 2 and 4 in B, samples 1 and 3 in C).

3c. Thin film sample preparation

Thin-film samples of were prepare by dissolving thymidine or thymidine-d_3 in methanol (Fisher, 0.01% H_2O) or d_4-methanol (Cambridge, 99.8% D). Approximately 200 µL of this solution was transferred to a quartz EPR sample tube. The methanol was pumped out from the sample tube under vacuum, leaving a thin film of thymidine, thymidine-d_3, or H/D-thymidine-d_3 on the bottom 3 cm of the sample tube. Removal of visible solvent required about 10 minutes under vacuum. The sample was then left for an additional 3 hours under vacuum to remove residual solvent. The EPR sample tube was then flame sealed under a low-pressure argon atmosphere.

4. Various models of the quantity of the d_3-TD radical in irradiated thy-d_3

There is a difference in yield of isotopologues even between similar preparations. In the context of spore photoproduct formation, the most important sample for determining the source of H atom donation to the C6 position of thymidine is the thymidine-d_3 sample. Presence of the d_3-TD radical indicates the methyl group of an adjacent thymidine is the donor of the additional hydron at the TH C6 position and supports the sequential radical pair mechanism for spore photoproduct formation discussed in the main text. Simulations (Figure S4, simulation parameters summarized in Table S3a and b) of the blue spectra (EPR at 120 K) in Figure S2C indicate that the ratio of d_3-TD radical varies slightly among different trials.

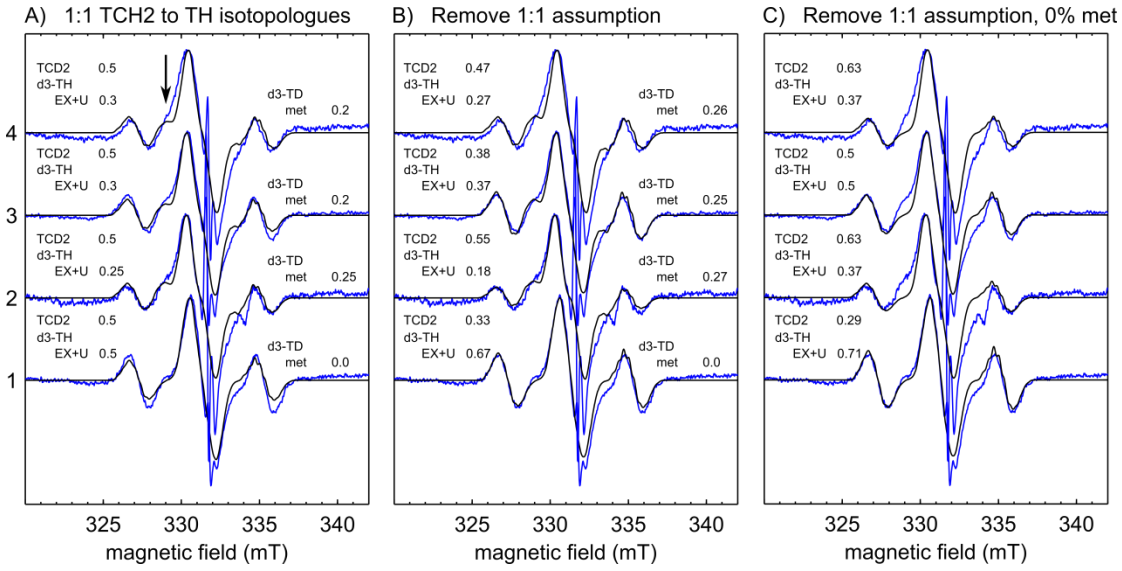

Figure S4. Three ways of simulating the blue spectra in Figure S2C (thy-d_3, UV irradiation temperature < 120 K, EPR temperature < 120 K) are shown. Experimental spectra are shown in blue and simulations in black. For thy-d_3 the oxidation product will be the TCD_2 isotopologue. The reduction products will be the d_3-TH isotopologue formed by the "EX" and "O" pathway and the d_3-TD radical formed by the "met" pathway (see main text for a discussion of the pathway abbreviations). A) First, using the restrictive scheme we assumed a 1:1 ratio of TCH_2:TH isotopologues. We find the percentage of d_3-TD in the simulation varies from 0 % to 25 % among the four trials. B) Next, we removed the 1:1 restriction which resulted in visually better simulations of the experimental data. In these simulations, the d_3-TD radical still made up between 0 % and 27 % of the radicals present among the four trials. C) Spectra are simulated by relaxing the assumption of a 1:1 ratio of TCH_2:TH isotopologues, but assuming no d_3-TD isotopologues are present (i.e. the "met" pathway of TH isotopologue formation is not active). In this case, the simulations for spectra 2-4 do not adequately model the spectral features we attribute to the d_3-TD radical present at 329 mT (marked by an arrow in A) and 334 mT. In A, B, and C simulation parameters (Table S3) are identical except for the ratio of TCH_2 and TH isotopologues included.

Table S3a: Simulation parameters for the TCD_2 isotopologue used in Figure S4[a,b,c]

species	g	g frame	H_{C6}	H_{C6} frame	H_{C7}	H_{C7} frame	H_{C7}	H_{C7} frame	$^{14}N1$	$^{14}N1$ frame	LWPP[d] (mT)
TCD_2	P	P	P	P	P·D	P	P·D	P	P	P	0.8

[a] "P" indicates the value is the same as the value for the primary isotopologue in the 3rd row of Table S1a

[b] P·D =P. $\gamma_{2_H}/\gamma_{1_H}$, D is the ratio of gyromagnetic ratios for ^2H and ^1H, approx. 0.1535

[c] All frames are the Euler angles of the rotation matrices computed in Orca

[d] Peak-to-peak line width

Table S3b: Simulation parameters for the TH isotopologues used in Figure S4 [a,b,c]

species	g	g frame	H_{C7} (methyl)	H_{C7} frame	H_{C6}	H_{C6} frame	H_{C6}	H_{C6} frame	LWPP[d] (mT)
TH-d_3	P	P	P·D	P	P	P	P	P	0.3
TD-d_3	P	P	P·D	P	P·0.75	P	P·D	P	0.3

[a] "P" indicates the value is the same as the value for the primary isotopologue in the 3rd row of Table S1b

[b] P·D =P· $\gamma_{2_H}/\gamma_{1_H}$, D is the ratio of gyromagnetic ratios for ^{2}H and ^{1}H, approx. 0.1535

[c] All frames are the Euler angles of the rotation matrices computed in Orca

[d] Peak-to-peak line width

5. Temperature dependence of radical signals in microcrystalline thymidine

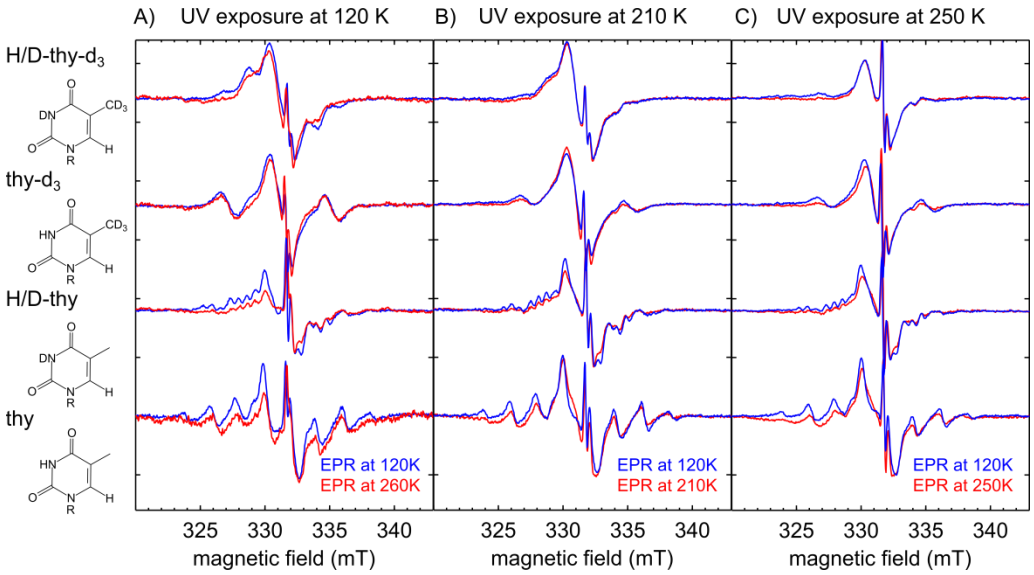

Figure S5: Shown in blue are the same spectra as in Figure 1 of the main text where EPR was recorded at 120 K. Shown in red is the EPR spectrum taken at a warmer temperature indicated in the figure (260 K in A, 210 K in B, and 250 K in C). In Figure S5A, after recording the EPR spectrum at 120 K, the sample was warmed to 250 K and the EPR spectrum recorded without any additional UV radiation applied. In Figure S5B, the sample was UV irradiated at 210 K and the EPR spectrum recorded. Then the sample was cooled to 120 K and the EPR spectrum was recorded without any additional UV radiation applied. In Figure S5C, the sample was UV irradiated at 250 K and the EPR spectrum recorded. Then the sample was cooled to 120 K and the EPR spectrum was recorded without any additional UV radiation applied. Spectrometer settings were as follows: microwave attenuation was 33 dB for spectra recorded below 120 K, 25 dB for spectra recorded at 210 K and 250 K; sweep rates of 40 seconds for 30 mT; microwave frequency between 9.302-9.336 GHz; modulation amplitude of 0.2 mT and frequency of 100 kHz; typically 30-100 scans were needed to achieve the signal to noise ratio of the spectra shown. In all cases the spectra were normalized to their most intense feature, so relative quantitation of number of radicals should not be made from this figure.

5a. Effects of warming samples UV irradiated at 120 K (Figure S5A)

The spectra of thymidine used in Figure S5A broadened upon warming but the position of the dominant features did not shift indicating no new radical species formed upon warming. The broadening is attributed to structural rearrangement of the radicals upon warming that could not occur at 120 K. This idea is substantiated by the EPR data collected on thin film samples of thymidine exposed to UV radiation. Thin film samples are more structurally amorphous than microcrystals and the spectra collected for thin film samples under identical UV irradiation were consistently broadened compared to microcrystalline samples of the same material (SI, Section 3).

Of particular importance is the broadening of the features due to the d_3-TD radical in thymidine-d_3 irradiated at 120 K upon warming to 250 K. These features at 329 and 333 mT broaden considerably upon warming, but look very similar to the spectra for thymdine-d_3 in Figure S5B where UV radiation was applied at 210 K. This supports our approach of simulating the spectra using the same isotopologues in different ratios at different temperatures, but simply broadening the features when UV radiation is applied at warmer temperatures (see simulation parameters in Tables S1a and S1b).

5b. Effects of cooling samples UV irradiated at 210 K and 250 K (Figures S5B and S5C)

In contrast to irradiating the samples at 120 K, each of the isotopically labeled thymidine starting materials was irradiated with UV light at 210 K and 250 K in Figure S5B and C, respectively. Cooling to 120 K increased the signal intensity and required data collection at lower microwave power to prevent saturation.

When thymidine-d_3 and H/D-thymidine-d_3 are irradiated and measured at warmer temperatures, the features due to the d_3-TH isotopologue at 327 and 336 mT are broadened nearly beyond detection, in particular in panel C. However, these features do sharpen and become detectable at 120 K. It is unexpected that in spectrum 4 of panel C there appears to be very little of the d_3-TD radical with features expected at 329 and 333 mT given it is so prominent in spectrum 4 in both panel A and B. However, this may be due to these broadening effects at warmer temperatures.

6. Graphical representation of pathway models

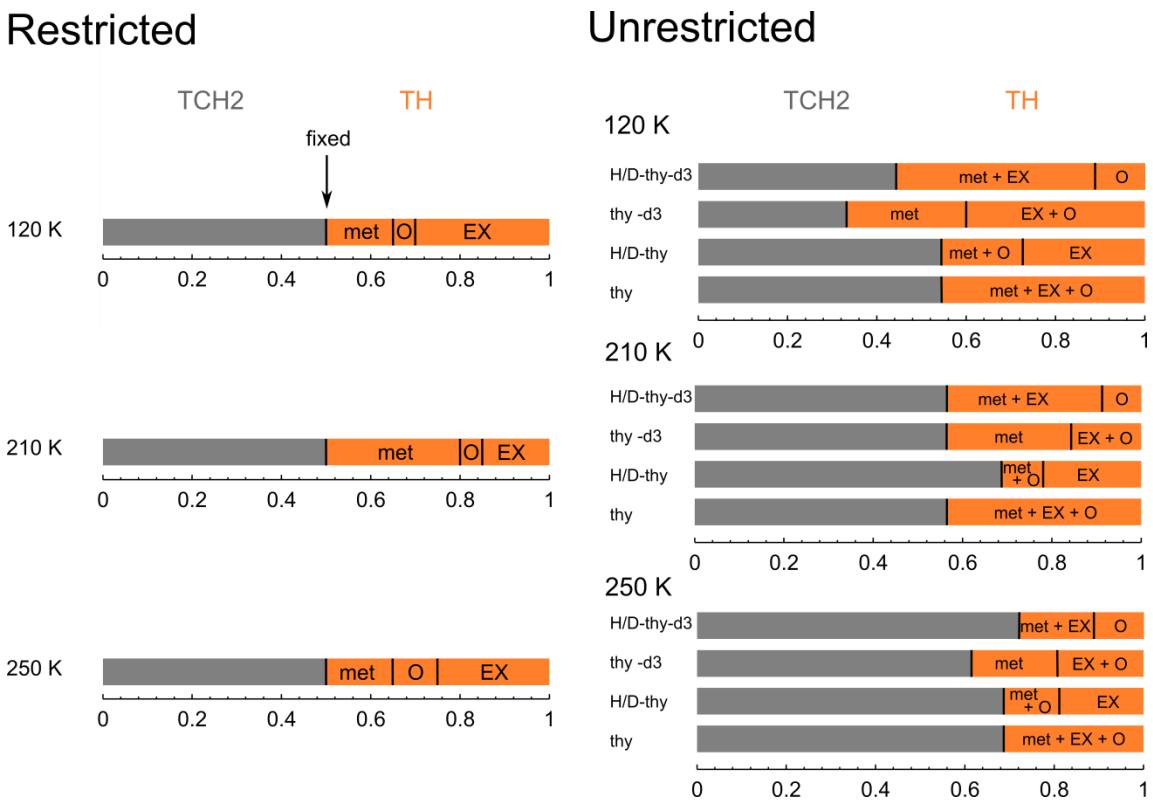

Figure S6. Left: A graphical representation of the restrictive model of radical formation in thymidine (with 1:1 restriction and isotope effect restriction, as defined in the main text) used in simulations shown in Figure 1. Right: A graphical representation of the unrestrictive model of radical formation in thymidine used in simulations shown in Figure S1. The gray bars represent the percentage of TCH_2 isotopologue present in each sample. The burnt-orange bars represent the percentage of TH isotopologues which form for a given pathway indicated by text in the figure. See the main text (results section) for a detailed account of which TH isotopologues will form for a given starting material and pathway.

7. Structures, property calculations, and simulations of EPR spectra of anion (T^-) and cation (T^+) thymidine radicals

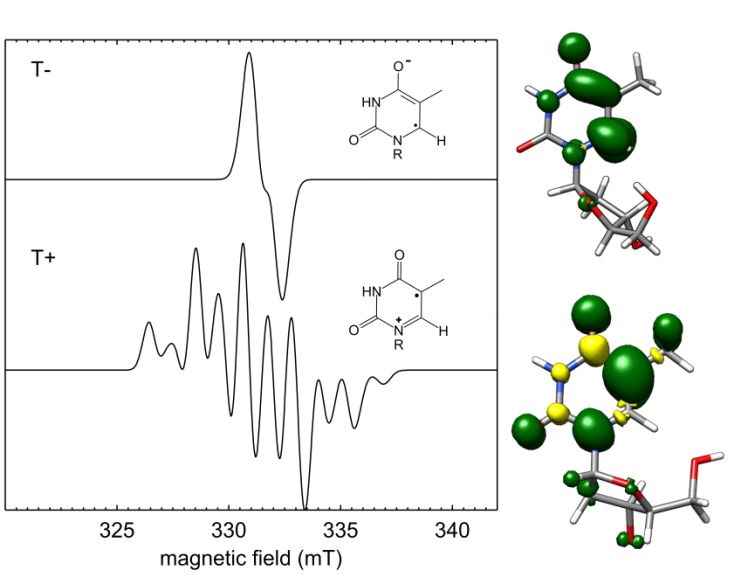

Figure S7: Simulations of the EPR spectra of the anion and cation radical formed from one electron reduction and oxidation of thymidine, respectively. EPR properties were calculated using the Orca 3.0 quantum computing software (details below). Simulations of the anion radical use the full g tensor and the hyperfine coupling of the proton at the N3 position, the proton at the C6 positon, and the methyl group protons at C5. Simulation of the cation radical use the full g tensor and hyperfine coupling tensors of the N1 nitrogen, the methyl group protons at C5, and the proton at the carbon bound to N1 (on the sugar moiety). In all cases the full tensors were used to account for the Euler angles between the principal values. Simulations used an arbitrary microwave frequency of 9.3 GHz in both cases. Principal values of the properties are listed in Table S4.

Table S4: Principal values of the calculated g tensor and hyperfine couplings (MHz) of the anion and cation thymidine radicals[a]

species	*g*	H_{C5} (methyl)[b]	H_{N3}	H_{C6}	LWPP (mT)
T^-	2.0023 2.0036 2.0047	2 3 8	1 -7 -7	7 -16 -36	0.6
	g	H_{C5} (methyl)[b]	$H_{C1'}$	N1	LWPP (mT)
T^+	2.0025 2.0053 2.0074	59 60 65	31 32 38	-0.5 -1 40	0.6

[a] Hyperfine coupling principal values are in MHz
[b] Average hyperfine coupling of the three methyl protons

Density Function Theory Calculations: Geometry optimization calculations were carried out using Gaussian09 software[1] with spin unrestricted orbitals, B3LYP functional, and 6-311++G basis set for the T^- radical and the 6-311G basis set for the T^+ radical. The magnetic properties including g-tensors and hyperfine coupling constants were calculated for the optimized geometries using ORCA 3.0[2] with spin unrestricted orbitals, the B3LYP functional, and 6-311G basis set for T^- and T^+. Simulations of EPR spectra were performed with the full 3×3 g and hyperfine tensors as input parameters to the EasySpin software. Only certain nuclei, indicated in Table S4, with substantial hyperfine coupling strengths were used in simulations. For the methyl group protons, the average of the full tensors was computed and used as the hyperfine coupling tensor for each of the three protons. The average principal values are reported in Table S4.

8. Exchange of protons in deuterated methanol

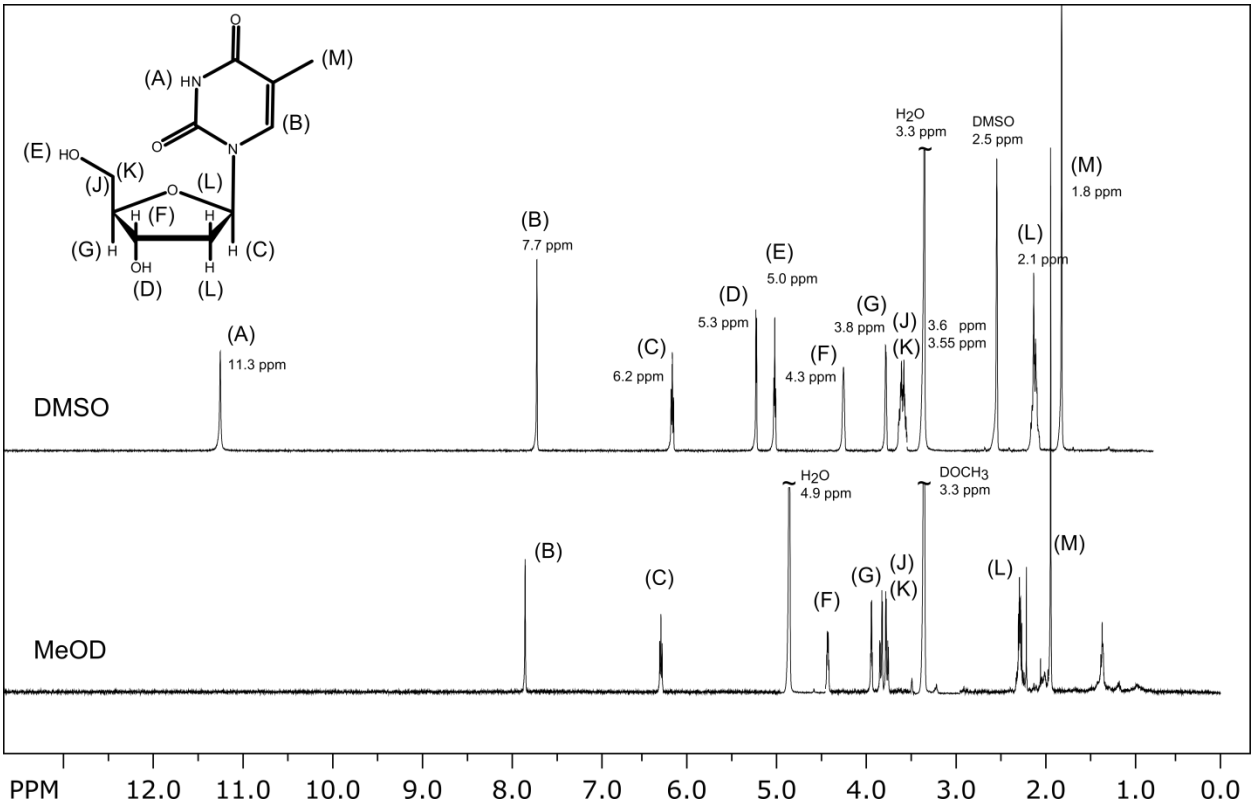

Figure S8: 499 MHz NMR of thymidine (structure in top left). Top spectrum: Thymidine in $(CD_3)_2SO$ (Cambridge Isotopes, 99.9%). The spectrum was assigned based on manufacturer and database spectra.[3,4] Bottom spectrum: Thymidine in $DOCD_3$ (Cambridge Isotopes, 99.8%). As can be seen by the disappearance of peaks (A), (D), and (E), the secondary amine and hydroxyl protons exchange readily in deuterated methanol. The intensity of solvent peaks denoted "~" were cut off for clarity.

9. References

(1) M. J. Frisch, G. W. Trucks, H. B. Schlegel, G. E. Scuseria, M. A. Robb, J. R. Cheeseman, G. Scalmani, V. Barone, B. Mennucci, G. A. Petersson, H. Nakatsuji, M. Caricato, X. Li, H. P. Hratchian, A. F. Izmaylov, J. Bloino, G. Zheng, J. L. Sonnenberg, M. Had, and D. J. F. Gaussian 09, Revision C.01, **2010.**

(2) Neese, F. The ORCA Program System. *WIREs Comput. Mol. Sci.* **2012**, *2*, 73–78.

(3) Ulrich, E. L.; Akutsu, H.; Doreleijers, J. F.; Harano, Y.; Ioannidis, Y. E.; Lin, J.; Livny, M.; Mading, S.; Maziuk, D.; Miller, Z.; *et al.* BioMagResBank. *Nucleic Acids Res.* **2008**, *36*, D402–D408.

(4) Thymidine(50-89-5)1HNMR, http://www.chemicalbook.com/SpectrumEN_50-89-5_1HNMR.htm.